APPLICATIONS OF SATELLITE ALTIMETRY TO OCEANOGRAPHY AND GEOPHYSICS

Robert E. Cheney
Bruce C. Douglas
David T. Sandwell
National Ocean Service, NOAA
Rockville, MD 20852

James G. Marsh
NASA Goddard Space Flight Center
Greenbelt, MD 20771

Thomas V. Martin
John J. McCarthy
EG&G Washington Analytical Services Center
Riverdale, MD 20737

Abstract

Satellite-borne altimeters have had a profound impact on geodesy, geophysics, and physical oceanography. To first order approximation, profiles of sea surface height are equivalent to the geoid and are highly correlated with seafloor topography for wavelengths less than 1000 km. Using all available Geos-3 and Seasat altimeter data, mean sea surfaces and geoid gradient maps have been computed for the Bering Sea and the South Pacific. When enhanced using hill-shading techniques, these images reveal in graphic detail the surface expression of seamounts, ridges, trenches, and fracture zones. Such maps are invaluable in oceanic regions where bathymetric data are sparse. Superimposed on the static geoid topography is dynamic topography due to ocean circulation. Temporal variability of dynamic height due to oceanic eddies can be determined from time series of repeated altimeter profiles. Maps of sea height variability and eddy kinetic energy derived from Geos-3 and Seasat altimetry in some cases represent improvements over those derived from standard oceanographic observations. Measurement of absolute dynamic height imposes stringent requirements on geoid and orbit accuracies, although existing models and data have been used to derive surprisingly realistic global circulation solutions. Further improvement will only be made when advances are made in geoid modeling and precision orbit determination. In contrast, it appears that use of altimeter data to correct satellite orbits will enable observation of basin-scale sea level variations of the type associated with climatic phenomena.

Marine Geophysical Researches 7 (1984) 17–32. 0025-3235/84/0071-0017$02.40.

A. Introduction

Satellite altimeters profile the sea surface with extraordinary precision (a few centimeters) and provide new ways of studying ocean circulation, the Earth's gravity, and its crustal structure. In the 5 years since Seasat, significant progress has been made in understanding and interpreting this new data type. Altimetric maps of mean sea height have revealed the intricate surface expression of trenches, ridges, seamounts, and fracture zones. Temporal variability of the sea surface due to meandering currents and eddies has been determined with an uncertainty of only a few centimeters, providing the first comprehensive view of the global eddy field. Even the broad, basin-scale circulation has been observed to a certain degree by subtracting the modeled gravimetric topography from global altimetric mean surfaces. In this brief article we present samples of these results derived from both Seasat and its predecessor, Geos-3.

B. Geophysics

Except for the 1 to 2 m surface topography associated with geostrophic flow and tides, the geoid and sea surface coincide. Altimeter data with a precision of 5 cm (Seasat) to 25 cm (Geos-3) can thus resolve geoid signals associated with seafloor topography. This precision, along with the dense ocean coverage afforded by these two satellites, enables construction of high resolution geoid maps over most ocean areas. In well surveyed areas, accurate geoid maps could be used to discriminate among the various modes of isostatic compensation of seafloor topography. They are even more useful in remote Southern Ocean areas since shorter wavelength geoid undulations can be used to map poorly surveyed and uncharted fracture zones (Sandwell and Schubert, 1982) as well as to locate and identify previously undetected large seamounts (Sandwell, 1984; Lazarewicz and Schwank, 1982). Moreover, orientations of fracture zones reflect relative plate motions in the past and place constraints on plate reconstruction models (Menard and Atwater, 1968). In addition to these geophysical applications, the maps are useful for geodesy. The two components of the deflection of the vertical are used for point positioning and inertial navigation.

Uncertainties associated with altimetric sea height measurements fall into several categories such as propagation errors and instrument noise, but these are dominated by radial ephemeris error which is usually of order 1 m. Fortunately, this error has a dominant period of once per revolution, so that over distances of a few thousand kilometers it can be well represented by a linear trend. Altimeter observations at ground track intersections (crossover points) provide one way of computing the correction to be applied to each profile. The technique of regional crossover adjustment to form highly precise mean sea surfaces has been described by Marsh et al. (1980).

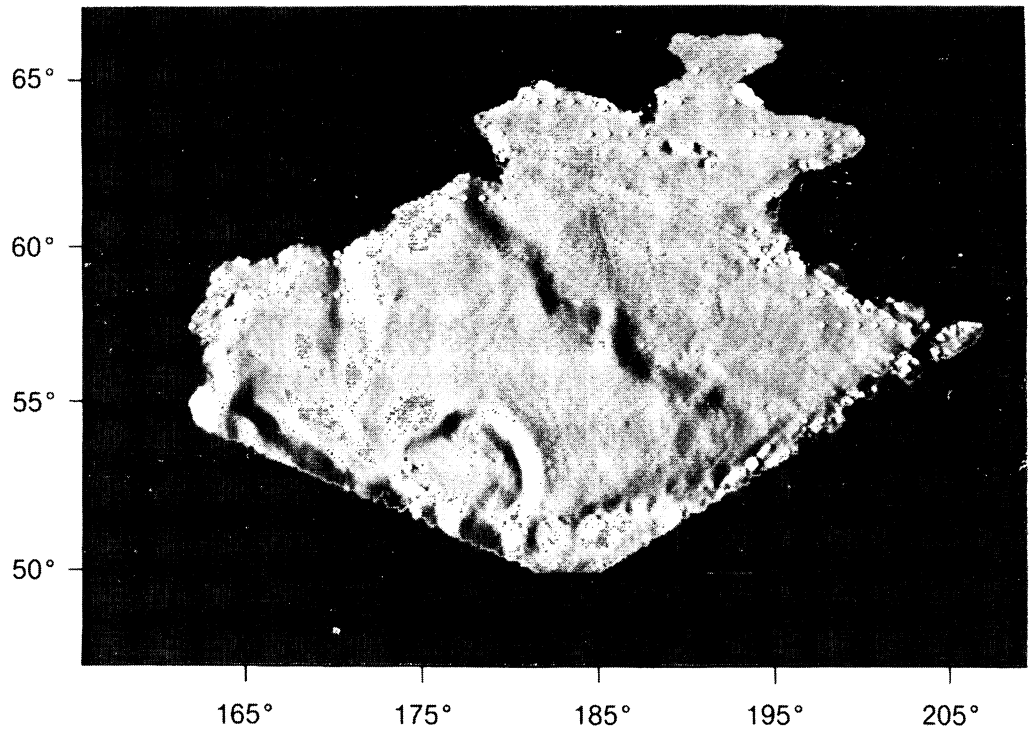

Figure 1. Mean sea surface of the Bering Sea computed from all available Geos-3 and Seasat altimeter data. The map has a resolution of approximately 15 km and a precision of about 15 cm. In this "sun-illumination" representation illumination is from the northeast (from Marsh et al., 1984).

Figure 1 shows the result after performing such an adjustment in the Bering Sea using all available Geos-3 and Seasat data. The map was first generated on a grid with a horizontal resolution of approximately 15 km. This was then transformed to a "sun-illumination" image by converting the horizontal gradients to grey shades. In this case, a northeast sun is casting shadows on the surface topography. The sharp gradient extending diagonally through the middle of the surface is the division between the shallow water over the continental shelf in the northeast and the deeper sea over the Bering Abyssal Plain in the southwest. Also visible are the Shirshov Ridge at 170 E longitude and Bowers Bank. A portion of the Aleutian Trench is seen at the southern edge of the map. A measure of the precision of this map is given by the 23 cm root-mean-square value of the nearly 17,000 crossover differences used in the adjustment. A more complete description of this work is provided by Marsh et al. (1984).

A second way of eliminating radial orbit error is to produce maps of geoid slope (deflection of the vertical) rather than geoid height. Typical values for orbit slope errors are of order 0.1 microradian while deflections of the vertical associated with short wavelength geoid topography are orders of magnitude larger. Thus when geoid slopes are used, orbit error is suppressed far below the typical geoid signals. Differentiation of each altimeter profile also acts as a high-pass filter, giving short wavelength geoid undulations about the same amplitudes as the long wavelength signals. A network of differentiated profiles can be used to construct deflection of the vertical maps and "sun-illumination" images. The example in Figure 2 is from the South Pacific. All existing Seasat and Geos-3 data in the region were used to compute deflections of the vertical on a 10 km grid, and an image was constructed simulating the sun shining on the sea surface. This area was chosen because it contains the Eltanin fracture zone system, the largest in the world, and because the area is poorly surveyed. Indeed, there are regions as large as 500 km by 500 km that contain no depth soundings.

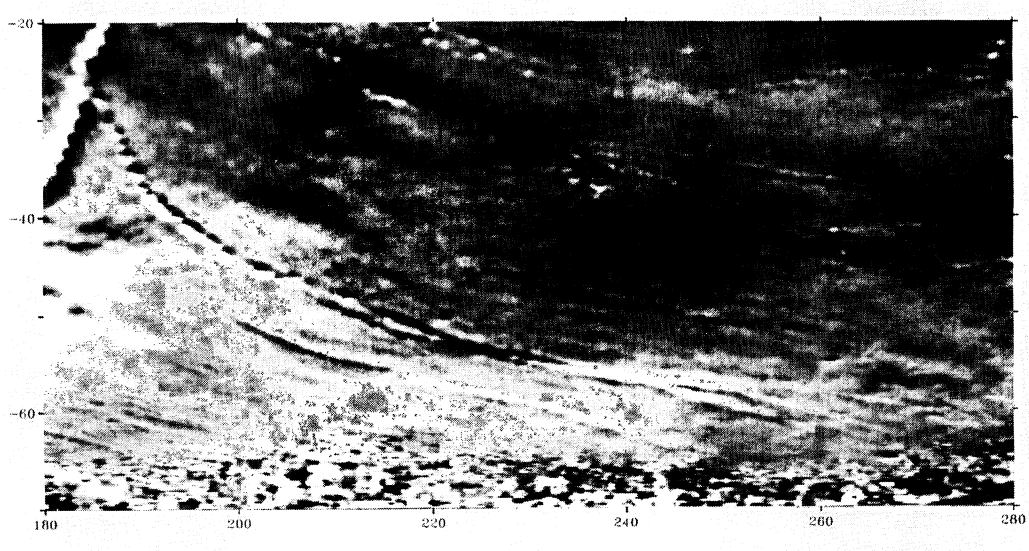

Figure 2. Geoid gradient map of the South Pacific using all available Geos-3 and Seasat altimeter data. Illumination is from the south, revealing the Heezen, Tharp, and Udintsev fracture zones. Also apparent are the Louisville Ridge and its connection with the Eltanin fracture zone system. Many seamounts are visible in the northeast (from Sandwell, 1983).

The image in Figure 2 is illuminated from the south and highlights the region north of the Eltanin fracture zone. (Sun azimuth and elevation can be varied to enhance different portions of the map.) The Eltanin fracture zone and Louisville Ridge are connected near 270 E, creating a continuous 5000 km feature. This connection was proposed by Hayes and Ewing (1968), but could not be confirmed until now because of the poor bathymetric coverage. The image also reveals approximately 200 large seamount signatures, half of which do not appear on published charts. A complete discussion of these results has been reported by Sandwell (1984).

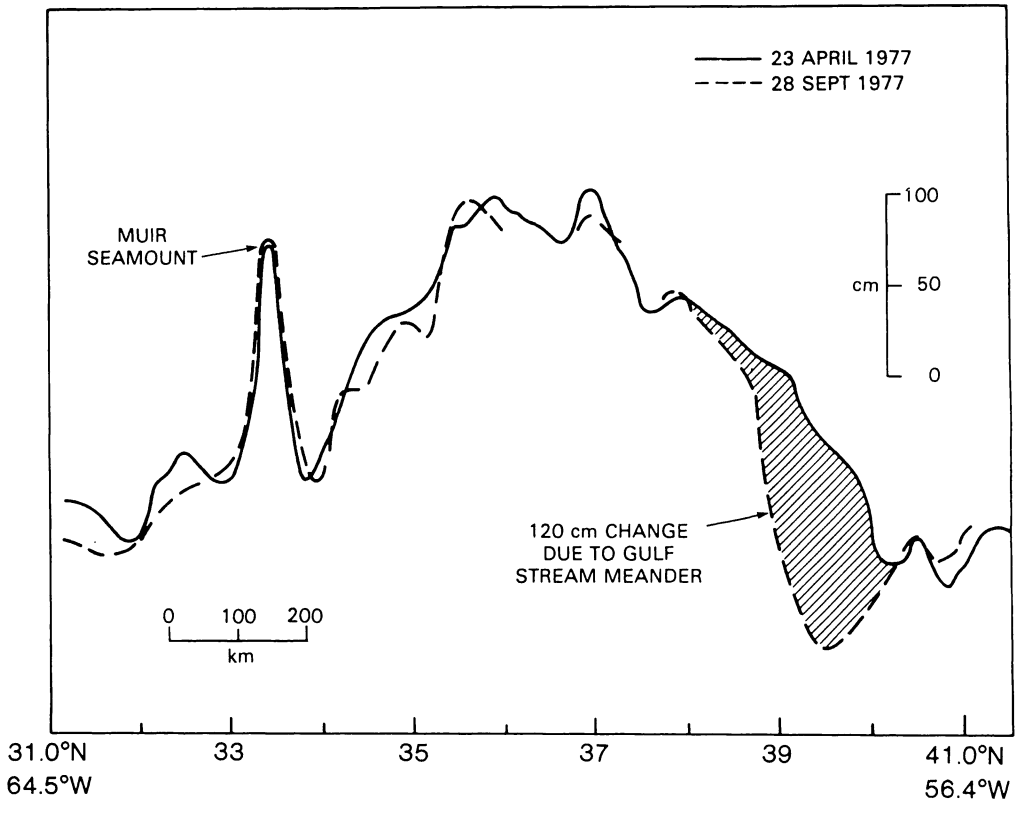

Figure 3. A collinear pair of Geos-3 altimeter profiles crossing the Muir seamount north of Bermuda. Note the identical geoid undulation in the profiles at the position of the seamount. The shaded area is the change in height due to a meander of the Gulf Stream (from Douglas et al., 1983).

C. Ocean Eddy Field

Geostrophic surface currents are maintained by horizontal pressure gradients and are expressed as sea height slopes relative to the geoid. While it is difficult to separate this dynamic component of sea height from the static geoid signal, an altimeter can readily detect the time-dependent variations in height. The most energetic fluctuations have typical scales of 100-300 km and are attributable to the ocean eddy field: meandering of narrow currents and migration of detached vortices. Eddying motions in the ocean are believed to be the dominant mechanism for transferring energy and momentum. Obtaining a basic description of the global distribution of mesoscale eddy variability is fundamental to an improved understanding of ocean dynamics.

The problem of radial orbit error must again be solved in computing mesoscale variability from altimeter data. The method demonstrated here employs profiles obtained along repeated ground tracks, for which the geoid contribution is the same. An example is shown in Figure 3. Two passes of Geos-3 data were taken along the same track in the North Atlantic but at different times. A linear trend has been removed from each profile to eliminate the long-wavelength orbit error. Each pass contains the same geoid profile, as demonstrated by the close agreement over the seamount. However, at the location of the Gulf Stream there is a difference of 120 cm due to a meander or shift in the current's position. Mesoscale variability can therefore be detected with pairs of altimeter passes having the same track.

This procedure is most applicable to the Geos-3 data which were collected in great volume in certain areas such as the North Atlantic. Even though Geos-3 did not have an orbit which repeated exactly at specific intervals, it did produce many pairs of profiles along the same ground tracks. Figure 4 is a map of sea height variability in the Gulf of Mexico and western North Atlantic derived from about 1000 collinear pairs of Geos-3 data collected over 3.5 years. These results show peaks of variability created by the Loop Current in the Gulf of Mexico and by the Gulf Stream east of Cape Hatteras. The least energetic area is south of 35°N. A more detailed discussion of these results, including comparisons with similar maps derived from standard oceanographic data, has been published separately (Douglas et al., 1983).

The technique of collinear differences has also been used to derive the global mesoscale variability from Seasat altimeter data (Cheney et al., 1983). In this case statistics were derived not from pairs, but from groups of collinear profiles accumulated during a 25-day period when the ground track was repeated at 3-day intervals. Variability was derived by computing the standard deviation of sea height every 7 km along the track from the series of eight or nine observations. Because of the relatively coarse cross-track grid described by the ground tracks (approximately 600 km at mid-latitudes) interpolation was required to compute values on a uniform global grid for contouring. The resulting map (Figure 5) displays patterns consistent with our present understanding

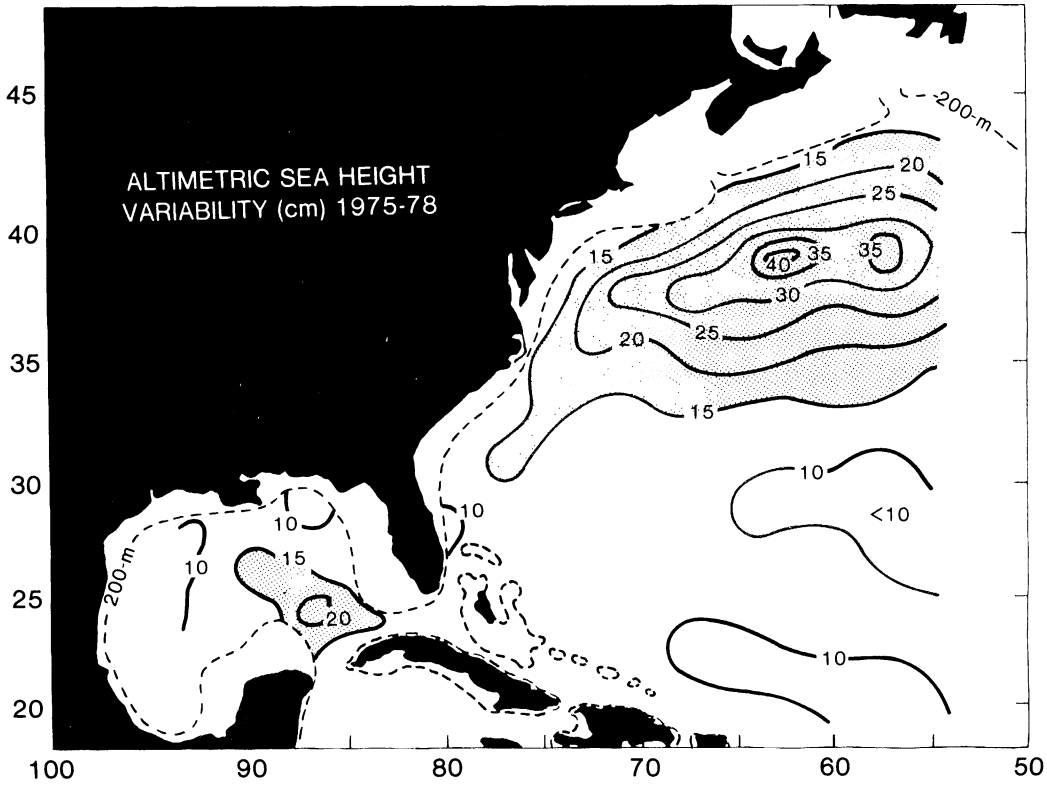

Figure 4. Mesoscale sea surface height variability in centimeters computed from repeated pairs of Geos-3 altimeter profiles during 1975-78. Maximum values are associated with the Loop Current in the Gulf of Mexico and the Gulf Stream meander region downstream of Cape Hatteras (from Douglas et al., 1983).

of the surface ocean circulation. In the North Pacific and the North Atlantic, the Kuroshio and Gulf Stream systems are represented as variability maxima extending 3000-4000 km into mid-ocean. The smoothing and interpolation process has damped their amplitudes down to about 10 cm from their actual along-track values of 20-30 cm, but they are still the dominant features of the Northern Hemisphere oceans. The North Equatorial Current systems are also associated with zonal bands of higher variability. The most prominent features in the Southern Hemisphere are the Agulhas Current off the tip of South Africa, the confluence of the Falkland and Brazil Currents east of Argentina, and the Antarctic Circumpolar Current, represented as a series of variability maxima surrounding Antarctica. Because of westward intensification of the wind-driven ocean currents, higher variability is most prevalent in the western parts of the oceans. This is best demonstrated in the Atlantic

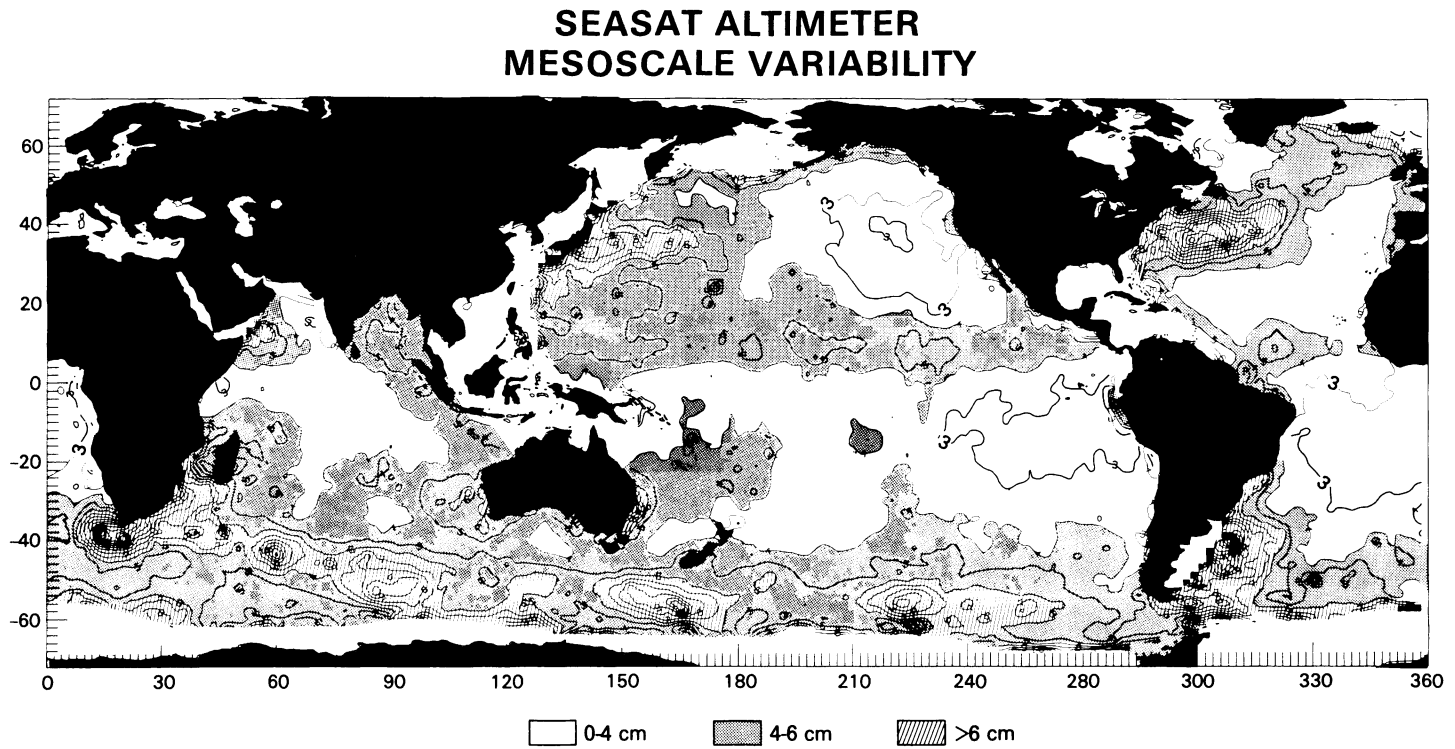

Figure 5. Global mesoscale sea height variability measured by the Seasat altimeter, September 15 to October 10, 1978. The North Atlantic and North Pacific are dominated by the highly energetic Gulf Stream and Kuroshio systems that extend seaward nearly 4000 km. In the southern hemisphere the Agulhas Current below Africa and the Falkland Brazil/Current confluence off South America are clearly apparent. High variability due to the Antarctic Circumpolar Current extends in a nearly continuous band through the polar oceans, with isolated maxima coinciding with major topographic ridges and plateaus. Owing to the predominance of values less than 4 cm in mid-ocean, the north equatorial current systems in both the Atlantic and Pacific can be seen as zonal bands of higher variability (from Cheney et al., 1983).

where the Northern and Southern Hemispheres are nearly mirror-images of each other. There is also a marked contrast between the highly variable western North Pacific and the quieter eastern basin, with the dividing line occurring near the Emperor seamount chain. This line of seamounts apparently acts as an efficient barrier to the high variability generated by the Kuroshio in the west. East-west asymmetry is characteristic of all oceans with values as small as 2-3 cm in the eastern parts of the major basins. Of all the global variability values computed, 70% were less than 5 cm, 26% were in the 5-10 cm range, and only 4% were greater than 10 cm. It is this broad background of low variability that permits some of the equatorial currents to be detected even though their dynamic height signatures are relatively small (25 cm).

One can carry the analysis of collinear altimeter data one step further and compute eddy kinetic energy. (See Menard, 1983, for derivation of the equations.) Although this merely involves computing the mean square deviation of sea surface slope, which is proportional to the variability of surface current speed, this calculation can only be made with collinear data. Variability solutions involving mean sea surfaces or crossover differences can produce results only in terms of sea height. Of course measurements along one track reveal only one component of the total geostrophic velocity, thus the eddy field must be assumed to be isotropic. The total eddy kinetic energy is then simply twice that observed along a single track. Figure 6 shows eddy kinetic energy for the North Atlantic computed from the Seasat collinear data. The pattern is nearly the same as in the height variability map. A peak of approximately 600 cm^2/s^2 is found in the Gulf Stream meander region. (As with the sea height variability shown in Figure 5, maximum values have been damped considerably by the interpolation and gridding process. Unsmoothed values of eddy kinetic energy in the Gulf Stream are approximately 2000 cm^2/s^2.) South of the Gulf Stream values decrease by an order of magnitude before increasing again to large values in the North Equatorial Current. Lowest values occur in the eastern North Atlantic. Similar distributions of energy have been derived from current measurements by ships and buoys. Although the Seasat results represent only a 25-day demonstration, future altimeters operating continuously for several years will be able to determine global eddy statistics with resolution and accuracy far exceeding that of standard oceanographic methods. (An exception to this statement is the calculation of eddy kinetic energy near the equator. To convert surface slope to current speed, one must divide by the Coriolis parameter, which varies as the sine of latitude and is zero at the equator. To make matters worse, computed geostrophic speeds must be squared to derive eddy kinetic energy. This puts a strict requirement on altimeter precision for profiles approaching the equator; any noise in measured sea height will be amplified and will appear as anomalous large energy. For the Seasat altimeter data, we have found that eddy energy values within approximately 1000 km of the equator are contaminated in this way. Evidence of this can be seen in Figure 6 in the vicinity of the North Equatorial Current where the rapid increase from 500 to greater than 1000 cm^2/s^2 is apparently due to altimeter noise and not eddy activity.)

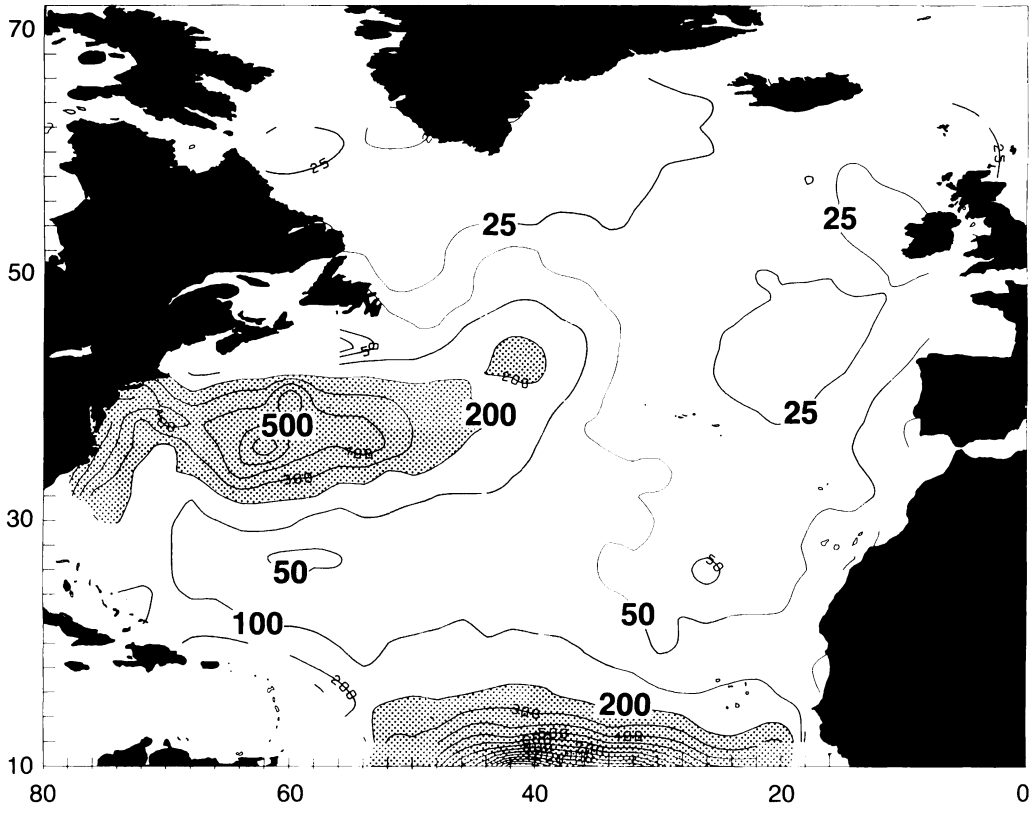

Figure 6. Eddy kinetic energy in the North Atlantic determined from the same Seasat collinear altimeter data used to derive the variability map in figure 5. Values are cm^2/s^2 and represent the mean square deviation of surface current speed as derived from the variability of sea surface slope. Maximum values are found along the Gulf Stream axis and in the region of the North Equatorial Current. Minimum eddy kinetic energy is found in the broad region extending from south of Bermuda northeast to Great Britain.

D. Large-scale Ocean Circulation

Ultimately it is believed that satellite altimetry will contribute to determination of the general circulation of the oceans (the long-term mean movement of water). In order to accomplish this, advances will be required in gravity field modeling and orbit determination. At the present time, uncertainties in these two areas are several times too large for reliable mapping of surface circulation. Recently, however, some surprisingly reasonable results have been obtained using existing

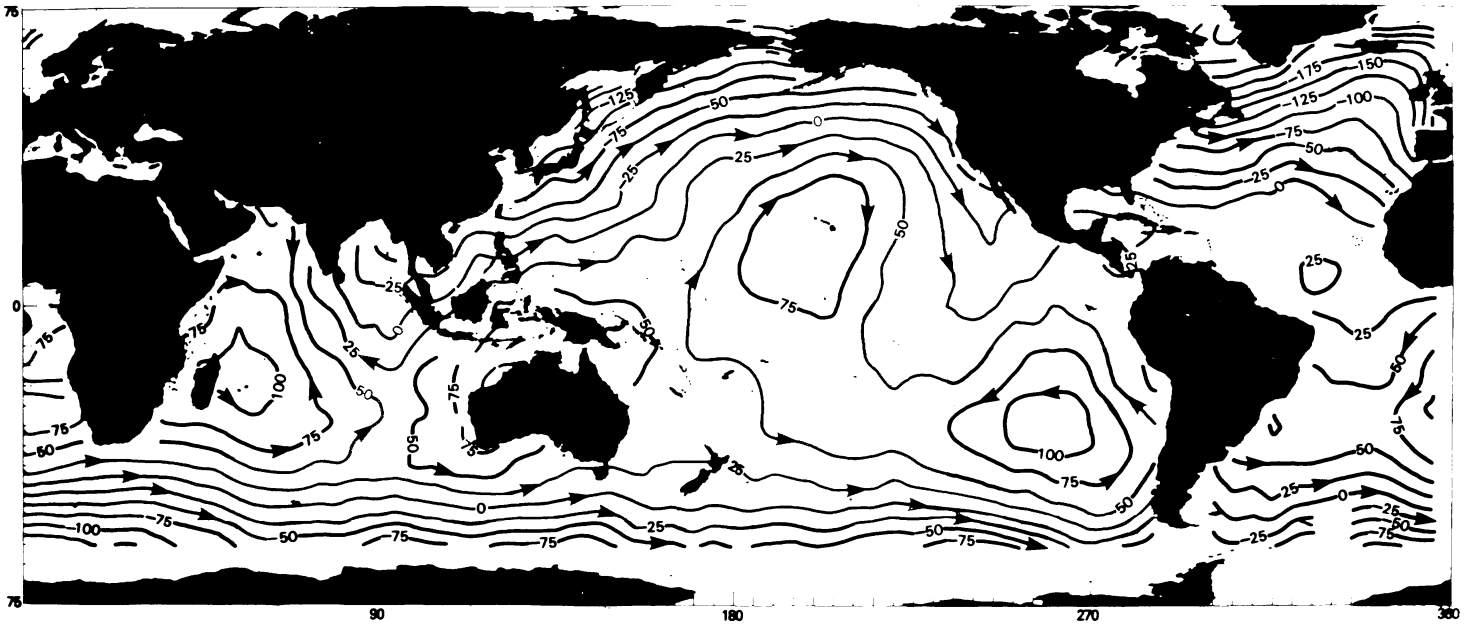

Figure 7. Dynamic topographic determined from altimetry. Contours in centimeters represent the differences between a long-term mean sea surface and a global geoid model. The surface consists of 1.5 years of Geos-3 data plus all existing Seasat altimetry. The geoid model, called PGS-S4, is based on a combination of satellite observational data, surface gravity, and also altimeter data. Both surfaces were smoothed before performing the difference to reveal only the large-scale (greater than 10,000 km) circulation features. Although certain aspects of the map are probably unrealistic, based on comparison with dynamic height maps from hydrography, gyres with the correct sense are found in the major ocean basins. A strong Antarctic Circumpolar Current is also apparent (from Cheney and Marsh, 1982).

altimeter data and geoid models (Cheney and Marsh, 1982; Tai and Wunsch, 1983, 1984; Douglas et al., 1984; Engelis, 1983). The example in Figure 7 displays the difference between a global altimetric mean surface and a geoid model. The mean sea surface was computed using 1.5 years of Geos-3 data and all 3 months of Seasat data. No attempt was made to explicitly correct for the long wavelength radial orbit error; however, it was thought that simple averaging over the 2-year span might produce a surface with good accuracy at the larger scales. The geoid model used was one generated to compute the most accurate orbits possible for Seasat (Lerch et al., 1982). The model, called PGS-S4, is based on the Goddard Earth Models but also contains Geos-3 and Seasat altimeter data. The altimeter data were weighted so that the higher degree and order terms of the geoid were improved (to 36,36) but the low terms were not significantly altered. Sea heights for the global mean surface and the geoid model were both computed on a 1 degree grid.

The residual map in Figure 7 was derived by subtracting the geoid from the altimetric surface. The residuals were then smoothed so that only features with scales greater than a few thousand kilometers were retained. (The filtering scheme has been described by Marsh and Martin 1982. The 1 degree resolution surfaces were recomputed on a 5 degree grid by fitting a bi-quadratic surface to each point based on data within a 20 degree radius.) This smoothing was necessary for two reasons. First, the altimetric surface contains much more resolution and detail than the 36,36 geoid model. Second, the Goddard geoid models are highly accurate at long wavelengths, but degrade rapidly for terms greater than 6,6 (Wagner and Lerch, 1978). Thus these geoid models can only be used to derive the largest scales of ocean circulation.

The residual sea height map in Figure 7 may be evaluated through comparison with maps of dynamic height calculated from shipboard measurements of temperature and salinity, e.g. those by Levitus (1982). There are many features of the altimetric solution that appear realistic. Sea height is 1-2 m higher at low latitudes than in subpolar seas. This establishes the well-known anticyclonic gyres in the major ocean basins. The simple fact that these gyres have the correct sense is highly encouraging. Details of their locations and magnitudes are of secondary importance. For example, in the altimetric solution, the North Pacific gyre is centered near Hawaii, while oceanographic charts show it more properly located south of Japan. Considering orbit and geoid uncertainties, such discrepancies are not unexpected. The altimetric solution does contain a strong, continuous current in the Southern Oceans much like the Antarctic Circumpolar Current. The ability of future geoid models and orbit determination techniques to improve this picture of the basin-scale circulation will be a demanding test of their absolute accuracy.

Temporal variability of the large-scale circulation is also important because of the link to weather and climate. An example is the El Nino/Southern Oscillation phenomenon in the Pacific. At approximately 5-year intervals, patterns of atmospheric pressure and wind in the tropics undergo dramatic change. Easterly trade winds normally create westward

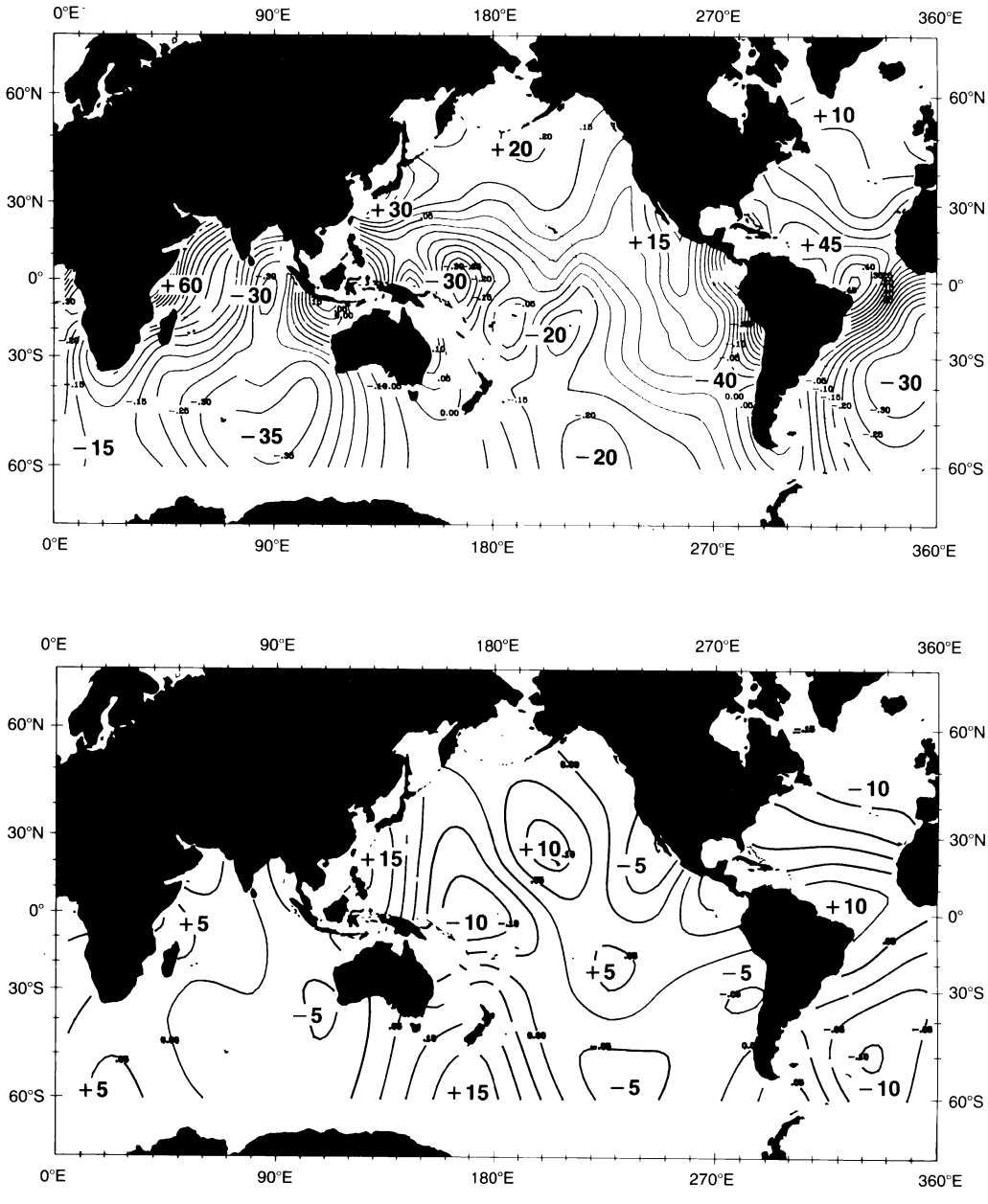

Figure 8. Apparent change in sea height between consecutive 3-day periods of Seasat altimeter data, September 15-17 and 18-20, 1978. In the upper map, standard orbits were used, and the differences represent the change in orbit error between the two periods. After correcting the orbit for each period independently using the altimeter data, the apparent change is reduced to less than 10 cm.

surface currents along the equator and set up a zonal gradient of sea height as water accumulates in the west. During El Nino, trade winds may actually reverse, resulting in a redistribution of water back toward the east. During the 1982-83 event sea level changes of up to 40 cm were observed near the equator. Even as far north as 45°N along the North American coast 35-cm monthly mean deviations were observed. These anomalous sea level signals apparently propagate eastward across the central Pacific over a period of a few months, but observations are limited to coastal and island tide gages. Documentation of the event in mid-ocean is therefore fragmentary. A satellite altimeter with a precision of a few centimeters can, in principle, provide a complete description of sea level change on all scales. However, determination of basin-scale changes is presently limited by uncertainty in the satellite position. The best ephemerides for Seasat still contain radial errors on the order of 50 cm.

A technique has been developed for correcting the radius of an altimetric satellite based on the altimeter data (Douglas et al., 1984). When modeled as a Fourier series the orbit error can be reduced to about 10 cm. While this technique does not necessarily determine the satellite position in an absolute reference frame, a time series of altimeter data can be made self-consistent, permitting observations of temporal sea height fluctuations on all scales. The procedure is best demonstrated using the Seasat collinear data when the ground track was repeated every 3 days. Because the distribution of data is the same for each 3-day set, temporal changes in sea level can be determined by subtracting one set from another. Figure 8 shows the observed change in sea height between two consecutive 3-day periods in September 1978. In only 3 days one would not expect to see large changes in sea height, yet significant differences are seen in Figure 8a in which standard Seasat orbits were used. Of course, these are not real differences; the map simply shows the change in radial orbit error between the two data sets. Figure 8b represents the same map after orbit corrections were applied using the Fourier approximation. Differences are now less than 10 cm in mid-ocean as expected. Some slightly higher values along continental boundaries are probably not meaningful due to the possibility of tidal contamination. Future altimeter missions with repeated ground tracks should therefore be capable of detecting decimeter basin-scale sea level changes even in the presence of substantially larger radial orbit uncertainty.

E. Conclusions

Precise profiling of the sea surface with satellite altimeters has proved to be invaluable for studies of the marine geoid, the Earth's crustal structure, and ocean circulation. With the dense coverage provided by the combined Geos-3 and Seasat data sets, high-resolution maps of the sea surface can be constructed. To an accuracy of a few percent, these surfaces are equivalent to the geoid and therefore are highly correlated with seafloor topography for wavelengths less than 1000 km. When these maps are enhanced using hill-shading techniques, they reveal in graphic

detail the structure of fracture zones, seamounts, ridges, trenches, and escarpments. In remote areas for which bathymetric data are sparse, altimetric maps represent an enormous improvement over existing charts and provide a basis for selecting future survey sites.

Altimetric determination of surface ocean circulation is inherently more difficult because of the relatively small signal amplitude. Dynamic topography must be separated from undulations of the geoid as well as from apparent undulations due to radial orbit error. For the case of mesoscale eddies, these obstacles have been completely overcome using repeated tracks of altimeter profiles from which geoid and orbit signals can readily be removed. This has resulted in highly accurate maps of sea height variability attributable to the ocean eddy field. Determination of absolute current velocities will require advances both in geoid modeling and in orbit determination. Some success has been attained, however, using existing geoids and global altimetric surfaces to compute the large-scale surface circulation. Nondynamical orbit correction schemes also appear promising for detection of large-scale sea height variability associated with important climatic phenomena such as El Nino.

Acknowledgements

Several others have been involved in the processing and analysis of the work summarized here. We thank Russell Agreen of NOAA National Geodetic Survey and Brian Beckley, Anita Brenner, and Hwa-ja Rhee of EG&G Washington Analytic Services Corporation.

References

Cheney, R.E. and J.G. Marsh: 1982, Global ocean circulation from satellite altimetry, Trans. Am. Geophys. Un., 63, p. 997.

Cheney, R.E., J.G. Marsh, and B.D. Beckley: 1983, Global mesoscale variability from collinear tracks of Seasat altimeter data, J. Geophys. Res., 88, pp.4343-4354.

Douglas, B.C., R.E. Cheney, and R.W. Agreen: 1983, Eddy energy of the northwest Atlantic and Gulf of Mexico determined from Geos-3 satellite altimeter data, J. Geophys. Res., pp. 9595-9603.

Douglas, B.C., R.W. Agreen, and D.T. Sandwell: 1984, Observing global ocean circulation with Seasat altimeter data, Marine Geodesy, in press.

Engelis, T.: 1983, Analysis of sea surface topography using Seasat altimeter data, Report 343 of the Department of Geodetic Science and Surveying, Ohio State University, Columbus, Ohio, 43210, 97 pp.

Hayes, D.E. and M. Ewing: 1968, The Louisville Ridge - A possible extension of the Eltanin fracture zone, Antarctic Res., 15, pp. 223-228.

Lazarewicz, A.R. and D.C. Schwank: 1982, Detection of uncharted seamounts using satellite altimetry, Geophys. Res. Lett., 9, pp. 385-388.

Lerch, F.J., J.G. Marsh, S.M. Klosko, and R.G. Williamson: 1982, Gravity model improvement for Seasat, J. Geophys. Res., 87, pp. 3281-3296.

Levitus, S.: 1982, Climatological atlas of the world ocean, NOAA Professional Paper 13, Rockville, MD, 20852.

Marsh, J.G. T.V. Martin, J.J. McCarthy, and P.S. Chovitz: 1980, Mean sea surface computation using Geos-3 altimeter data, Mar. Geod., 3, pp. 359-378.

Marsh, J.G., R.E. Cheney, J.J. McCarthy, and T.V. Martin: 1884, Regional mean sea surfaces based upon Geos-3 and Seasat altimeter data, Mar. Geod., in press.

Marsh, J.G. and T.V. Martin: 1982, The Seasat altimeter mean sea surface model, J. Geophys. Res., 87, pp. 3269-3280.

Menard, Y.: 1983, Observations of eddy fields in the northwest Atlantic and northwest Pacific by Seasat altimeter data, J. Geophys. Res., 86. pp. 8022-8030.

Menard, H.W. and T.M. Atwater: 1968, Changes in direction of sea floor spreading, Nature, 219, pp. 463-467.

Sandwell, D.T.: 1984, A detailed view of the South Pacific geoid from satellite altimetry, J. Geophys. Res., in press.

Sandwell, D.T. and G. Schubert: 1982, Geoid height versus age for symmetric spreading ridges, J. Geophys. Res., 85, pp. 7235-7241.

Tai, C.K. and C. Wunsch: 1983, Absolute measurement by satellite altimetry of dynamic topography of the Pacific Ocean, Nature, 301, pp. 408-410.

Tai, C.K. and C. Wunsch: 1984, An estimate of global absolute dynamic topography, J. Phys. Oceanogr., in press.

Wagner, C.A. and F.J. Lerch: 1978, The accuracy of geopotential models, Planet. Space Sci., 26, pp. 1081-1140.